Alpha-Gamma Angular Correlations in ^{12}C, ^{24}Mg, ^{58}Ni, and ^{120}Sn

N. Baron, R. F. Leonard, and W. M. Stewart
National Aeronautics and Space Administration, Lewis Research Center, Cleveland, Ohio 44135
(Received 12 March 1971)

The angular correlation between inelastically scattered α particles and the subsequent de-excitation γ ray has been measured at an α energy of 42 MeV. Measurements have been carried out in the reaction plane for γ rays resulting from the decay of the first excited (2^+) state of ^{12}C, ^{24}Mg, ^{58}Ni, and ^{120}Sn. The results are reported in terms of the γ-ray symmetry angle, θ_0, and the ratio A/B. Qualitatively the behavior of the symmetry angle is found to be the same for all four isotopes, rotating continuously at forward α-scattering angles and oscillating about the plane-wave and adiabatic predictions at larger α-scattering angles. For the three isotopes for which A/B measurements were possible, the ratio was clearly not identically zero. Both the angular-correlation and cross-section data are compared with the results of distorted-wave–Born-approximation calculations using a wide range of optical-model parameters. The optical-model ambiguities encountered here are similar to those found in fitting cross-section data alone.

I. INTRODUCTION

The measurement of differential cross sections for the inelastic scattering of medium-energy α particles has been extensively investigated.[1,2] Such measurements, however, yield only a limited amount of information, since the cross section depends only on the sum of the squares of the absolute magnitudes of magnetic-substate transition amplitudes. To completely describe the scattering to a 2^+ state, however, 10 numbers are required (either the magnitudes and phases of the five substate transition amplitudes or, equivalently, the magnitudes and phases of the five components of the nuclear-polarization tensor following the scattering). In reality, the symmetries of the problem[3] reduce the number of required parameters to only five plus an over-all phase angle. In principle all of these may be determined by measuring the α-γ correlation both in and out of the reaction plane.[4] For measurements in the reaction plane, the form of the correlation function permits determination of only two of the five possible parameters (unless absolute γ-ray count rates are measured). The physical significance of the measured parameters (A/B and θ_0) is most easily expressed in the notation of Cramer and Eidson.[4]

$$A/B = (1 - a_2)^2/4a_2 , \tag{1}$$

$$\theta_0 = \tfrac{1}{4}\delta_2 , \tag{2}$$

where a_2 and δ_2 are the relative magnitude and phase of the $m=2$ component of the polarization tensor as expressed in the coordinate system of Ref. 4. Earlier measurements have already established that the simpler theories[5-7] of α scattering are inadequate for the description of the angular correlation, even though both of these models are fairly accurate in their prediction of scattering cross sections. This earlier experimental work was carried out at lower energies (22.5 MeV) over a wide angular range,[8,9] and at 42 MeV over a rather limited angular range.[10,11] The present work was undertaken for two purposes. The first was to determine whether the additional information obtained from in-plane correlations would be helpful in resolving the optical-potential ambiguities[12-14] normally encountered in studies of α-scattering cross sections. The second objective was the further study of some of the simpler models of α scattering. In particular, additional data would help to determine whether there exist any cases in which the adiabatic and plane-wave Born approximations can correctly predict the in-plane correlation pattern. Also, there are several models[15,16] which give reasonable descriptions of existing angular-correlation data. The present study will further test those descriptions at higher energies, at larger angles, and on heavier nuclei.

II. EXPERIMENTAL ARRANGEMENT

For the experiments reported here the external 42-MeV α-particle beam of the National Aeronautics and Space Administration Lewis Research Center 1.5-m cyclotron was used. Two slightly different beam-handling systems, one of which is shown in Fig. 1, were used in the course of the experiment. In both arrangements, reduction of γ-ray background in the room was of primary concern, therefore the last slit defining the incident beam direction was 327 cm from the target and shielded from the γ detector by approximately 90 cm of lead and concrete. The beam stopper was

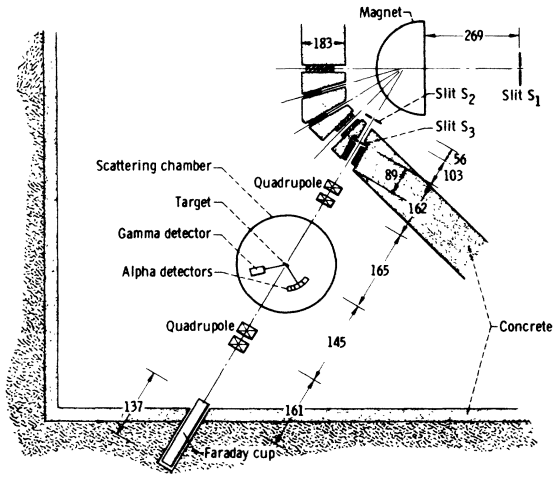

FIG. 1. Schematic diagram of scattering system. (All dimensions are in cm.)

located 137 cm within the rear wall of the room and was 440 cm from the target. The other beam-handling system differed from the one shown in Fig. 1 only in that the beam was stopped at the center of a 76-cm-diam by 152-cm-long tank of boron-loaded water. This tank was located approximately 213 cm from the target and was shielded from the γ detector by 30 cm of lead and concrete. Both systems utilized a 1.5-m-diam scattering chamber, which was large enough to contain the γ detector.

For all the work reported here the same type of detectors was used. The α detectors were lithium-drifted silicon, used in an array with a 4° spacing between detectors. The full angular resolution of each detector was usually 1°, although some forward-angle runs on nickel and tin were done with an angular resolution of $\frac{1}{4}$°. The γ detector used was a 7.62 by 7.62-cm sodium iodide crystal integrally mounted on an RCA 8054 photomultiplier tube and encased in a 0.64-cm-thick lead shield. The γ detector was placed $12\frac{1}{2}$ cm from the target so that it subtended a full angle of 35° and covered about 2.2% of the total sphere. All of the targets were self-supporting, about 1 mg/cm^2 thick, and except for ^{12}C were isotopically enriched.

Two different sets of electronics were employed. In one arrangement only three α detectors were used with separate amplifiers and coincidence circuits for each, the α-energy signals being combined just before entering a 1024-channel pulse-height analyser (PHA). In the other arrangement, 16 α-particle detectors were used and the signals from their preamplifiers were added, with all sixteen utilizing a common linear amplifier, biased amplifier, and coincidence circuit. This is shown schematically in Fig. 2. In both arrangements the

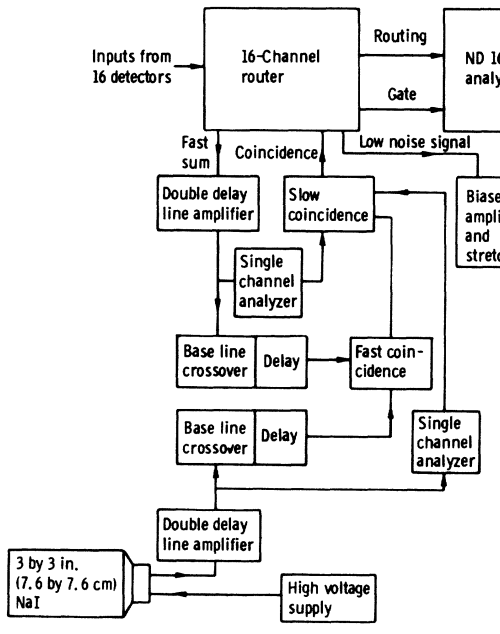

FIG. 2. Multidetector coincidence arrangement using 16-channel router.

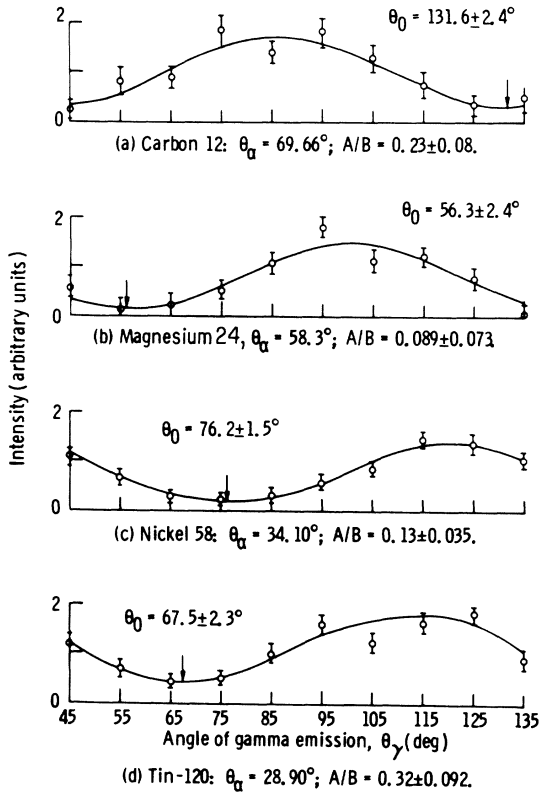

FIG. 3. Typical correlation patterns with least-squares fits to the function $W(\theta_\gamma) = A + B \sin^2 2(\theta_\gamma - \theta_0)$. Ratios of the isotropic to anisotropic component as presented were not corrected for finite geometry.

coincidence circuit was a standard parallel fast-slow arrangement with fast input signals being derived from cross-over timing and the slow inputs being derived from single-channel analyzers which guaranteed that both the α and γ signals fell within the energy range of interest. The resolving time of the fast-coincidence circuit was 50 nsec. In both cases if all the coincidence requirements were satisfied the PHA then analyzed the α-particle energy pulse, storing it in a proper segment of the 4096-channel memory. By comparing the α-particle spectra thus obtained with those obtained without any coincidence requirement, it was possible to correct for random coincidences and determine the true coincidence rate.

Data were obtained by fixing the angles of all the α detectors employed and varying the position of the γ detector in 10° steps between 45 and 135°. The coincidence data obtained were normalized relative to a monitor α detector fixed at a scattering angle of approximately 35° below the incident beam in the forward direction.

More detailed descriptions of the experimental arrangements used for individual isotopes have been given elsewhere.[17-20]

TABLE I. Experimental results of $^{12}C(\alpha,\alpha'\gamma\ 4.433$ MeV) angular correlation.

α-particle c.m. scattering angle, θ_α (deg)	γ-ray symmetry angle, θ_0 (deg)	Ratio of isotropic to anisotropic component, A/B
26.55	7.81 ± 2.43	0.13 ± 0.07
29.18	23.60 ± 1.90	0.26 ± 0.07
31.80	47.06 ± 2.42	0.25 ± 0.07
34.41	60.47 ± 1.74	0.12 ± 0.05
37.01	66.27 ± 5.33	0.00 ± 0.03
39.60	71.53 ± 1.02	0.00 ± 0.03
42.18	78.60 ± 2.17	0.024 ± 0.058
44.75	85.71 ± 1.60	0.00 ± 0.03
47.31	3.38 ± 1.72	0.00 ± 0.03
49.85	15.20 ± 1.87	0.13 ± 0.06
52.38	35.02 ± 5.20	0.31 ± 0.18
54.90	51.48 ± 4.48	0.22 ± 0.14
57.40	63.86 ± 3.40	0.097 ± 0.098
59.88	64.12 ± 3.30	0.35 ± 0.13
62.35	61.21 ± 7.90	2.0 ± 1.2
64.80	31.97 ± 3.48	0.41 ± 0.14
67.24	38.99 ± 2.34	0.079 ± 0.069
69.66	41.57 ± 2.42	0.14 ± 0.07
72.05	51.16 ± 1.21	0.061 ± 0.035
74.43	54.52 ± 1.84	0.13 ± 0.05
76.79	60.75 ± 2.86	0.083 ± 0.081
79.13	51.57 ± 3.01	0.60 ± 0.14
81.45	57.25 ± 2.89	0.24 ± 0.09
83.74	55.47 ± 2.17	0.34 ± 0.08
86.01	57.23 ± 5.44	0.41 ± 0.22
88.27	56.56 ± 2.56	0.093 ± 0.072
90.50	53.69 ± 1.14	0.059 ± 0.032
94.88	60.73 ± 1.27	0.00 ± 0.03

III. EXPERIMENTAL RESULTS

A. Correlation Measurements

For the sequence of spins investigated here ($0^+ \rightarrow 2^+ \rightarrow 0^+$) the form of the correlation function in the scattering plane for a fixed value of the α-scattering angle is known to be[21]

$$W(\theta_\gamma) = A + B \sin^2 2(\theta_\gamma - \theta_0) . \quad (3)$$

In this expression and elsewhere in this report, the data are defined relative to a spherical-coordinate system with the polar axis along the incident beam direction and the α-particle scattering defined as being at the azimuthal angle $\phi_\alpha = 0°$. Relative to this coordinate system, all of the measurements reported here are at an azimuthal γ-angle $\phi_\gamma = \pi$. Using the method of least squares the experimental data were fit with the function (3). Typical results for each isotope are shown in Fig. 3. The resulting values of A/B and θ_0 were then corrected for the effect of the finite size of the γ detector, using the method described by Rose[22] and Eidson *et al.*[8] Geometrical corrections leave the symmetry angle θ_0 unchanged but result in a decrease of the ratio A/B. The results for all four isotopes (after geometrical corrections) are listed in Tables I–IV. At angles where there existed overlap with earlier data[10, 11] good agreement was obtained. All four of the isotopes studied exhibit a qualitatively similar behavior. At forward α-scattering angles, the symmetry angle rotates continuously, crossing the adiabatic prediction at angles corresponding to maxima in the inelastic cross section and showing maximum departure from the adiabatic prediction where the inelastic cross section is a minimum. At larger scattering angles the continuous rotation is replaced by an oscillation about the adiabatic prediction, although the maximum deviation still seems to occur at the minima in the scattering cross section. It is more difficult to generalize in describing the behavior of the ratio A/B. This is due in part at least to the relatively large errors involved in the measurement of this parameter. It is clear, however, that at least for ^{12}C, ^{24}Mg, and ^{58}Ni the measured ratio is sometimes larger than zero, the value predicted by both the plane-wave Born approximation and the adiabatic approximation. This indicates that for all three isotopes there exists some polarization of the residual nucleus in a direction perpendicular to the reaction plane. Because of the large errors associated with the mea-

sured values of this parameter and the generally poor quality of fits to them, no comparison between calculations and A/B ratios will be shown. Unfortunately, experimental difficulties prevented measurement of the A/B ratio for ^{120}Sn. Data for this isotope were more difficult to obtain, principally because of the large γ background produced by the target. γ rays from competing α-induced reactions were so intense that it was impossible to observe the 1.17-MeV photopeak in the γ-ray singles spectrum.

All of the present data are shown, together with the adiabatic prediction, the plane-wave Born prediction, and the data of Refs. 10 and 11 in Figs. 4–7.

TABLE II. Experimental results of ^{24}Mg(α, α' γ 1.37 MeV) angular correlation.

α-particle c.m. scattering angle, θ_α (deg)	γ-ray symmetry angle, θ_0 (deg)	Ratio of isotropic to anisotropic component, A/B
18.70	84.4 ± 1.7	0.30 ± 0.06
21.03	17.8 ± 4.4	0.79 ± 0.29
23.35	68.0 ± 2.2	0.28 ± 0.08
25.67	72.1 ± 0.8	0.14 ± 0.02
27.98	69.3 ± 2.8	0.16 ± 0.07
29.14	72.3 ± 0.9	0.081 ± 0.027
32.60	73.0 ± 2.5	0.11 ± 0.05
34.90	66.3 ± 3.0	0.070 ± 0.05
37.19	68.2 ± 1.8	0.097 ± 0.06
39.48	63.2 ± 1.8	0.083 ± 0.04
41.76	65.0 ± 2.2	0.13 ± 0.05
44.04	68.0 ± 2.3	0.11 ± 0.05
46.30	67.0 ± 3.0	0.068 ± 0.05
48.56	54.3 ± 2.0	0.04 ± 0.05
49.35	61.4 ± 8.3	1.6 ± 1.00
50.81	57.6 ± 1.0	0.045 ± 0.05
53.06	56.0 ± 1.0	0.19 ± 0.11
53.84	54.9 ± 3.5	0.12 ± 0.10
55.29	57.4 ± 2.5	0.027 ± 0.040
57.52	56.4 ± 3.2	0 ± 0.10
58.30	56.3 ± 2.4	0.059 ± 0.07
59.73	60.0 ± 1.0	0.011 ± 0.065
61.94	60.1 ± 1.6	0.19 ± 0.13
62.71	62.2 ± 3.3	0.31 ± 0.12
64.14	51.3 ± 1.2	0.13 ± 0.04
66.33	45.9 ± 2.9	0 ± 0.09
67.09	48.3 ± 2.8	0.16 ± 0.08
68.51	48.0 ± 2.2	0.059 ± 0.05
70.67	41.5 ± 2.9	0 ± 0.13
72.83	48.1 ± 2.6	0.29 ± 0.10
74.98	61.9 ± 1.3	0 ± 0.06
75.74	50.7 ± 7.7	0.27 ± 0.24
77.11	48.1 ± 3.0	0.026 ± 0.081
79.24	61.7 ± 3.5	0.48 ± 0.16
79.98	60.7 ± 6.6	0.56 ± 0.33
81.35	34.4 ± 6.4	0.097 ± 0.070
83.45	43.3 ± 8.6	0.35 ± 0.04
84.19	34.7 ± 23.1	0.79 ± 1.40
85.54	50.6 ± 5.5	0.093 ± 0.12
88.34	31.3 ± 12.4	0.79 ± 0.80
89.68	53.5 ± 4.7	0 ± 0.12
92.45	49.9 ± 5.0	0 ± 0.16
93.78	71.6 ± 18.8	0.21 ± 0.53

B. Cross-Section Measurements

For each of the isotopes it was necessary to have cross-section measurements with which to compare the results of any calculations which might be performed. For carbon and nickel, measurements were available,[23–25] but not at exactly the energy at which the correlation experiments were done. For this reason the cross sections for elastic scattering and inelastic scattering to the first excited state were measured for these two isotopes. The experimental arrangement for these measurements is essentially that which has been described previously.[26] For ^{12}C, the cross-section data obtained[18] are in reasonable agreement with those which have previously been measured,

TABLE III. Experimental results of ^{58}Ni(α, $\alpha'\gamma$ 1.452 MeV) angular correlation.

α-particle c.m. scattering angle, θ_α (deg)	γ-ray symmetry angle, θ_0 (deg)	Ratio of isotropic to anisotropic component, A/B
12.82	76.4 ± 5.2	0.52 ± 0.25
14.96	83.9 ± 3.7	0.16 ± 0.10
16.02	81.9 ± 4.3	0.12 ± 0.12
18.16	60.7 ± 3.5	0.038 ± 0.098
19.22	80.9 ± 4.1	0.29 ± 0.13
20.29	72.8 ± 2.2	0.19 ± 0.07
21.35	76.4 ± 2.8	0.11 ± 0.08
22.42	77.6 ± 3.3	0.10 ± 0.09
23.48	76.3 ± 2.0	0.042 ± 0.059
24.55	82.1 ± 3.1	0.079 ± 0.085
25.61	79.5 ± 4.2	0.11 ± 0.09
26.67	5.3 ± 7.7	0.088 ± 0.21
27.73	11.1 ± 6.0	0.76 ± 0.75
29.86	69.8 ± 2.7	0.022 ± 0.074
31.98	75.2 ± 2.9	0.16 ± 0.06
34.10	76.2 ± 1.5	0.052 ± 0.043
36.21	66.1 ± 7.5	0.23 ± 0.12
40.44	57.4 ± 7.9	0.34 ± 0.29
42.54	68.1 ± 2.3	0.0 ± 0.17
44.65	76.6 ± 6.0	0.021 ± 0.17
46.75	64.5 ± 6.7	0.0 ± 0.23
48.85	68.1 ± 56.4	1.4 ± 6.2
50.94	61.3 ± 10.2	0.24 ± 0.34
53.03	57.3 ± 9.1	0.27 ± 0.30
55.12	60.7 ± 7.7	0.0 ± 0.22

although the maximum in the inelastic scattering observed near 55° by Naqib[23] is not as pronounced. This difference may be attributed to the small difference in the incident α-particle energy. At backward angles the data are reasonably similar to those of Yavin and Farwell.[24] A similar result is found when comparing the present ^{58}Ni data[19] with that of Ref. 25. For scattering from magnesium[27] and tin[26] the cross sections had previously been measured with the Lewis Research Center cyclotron.

IV. DWBA CALCULATIONS WITH COLLECTIVE FORM FACTORS

For each of the isotopes studied optical-model distorted-wave Born-approximation (DWBA) calculations were performed using the computer codes SCAT4[28] and DRC.[29] The optical potential used is given by

$$U(r) = V_C(r) - Vf(r, r_0, a_0) - iWf(r, r_i, a_i), \quad (4)$$

where $V_C(r)$ is the Coulomb potential between the incident α particle and the scattering nucleus, which is assumed to be a uniformly charged sphere of radius $1.25A^{1/3}$ F, and $f(r, r_x, a_x)$ denotes the Woods-Saxon radial form factor and has the form

$$f(r, r_x, a_x) = \left[1 + \exp\left(\frac{r - r_x A^{1/3}}{a_x}\right)\right]^{-1}. \quad (5)$$

The original DRC program has been modified to allow the calculation of angular correlations as well as inelastic cross sections. For all of the DWBA calculations, the nucleus was treated in terms of a macroscopic collective model.

TABLE IV. Experimental results of ^{120}Sn($\alpha, \alpha'\gamma$ 1.176 MeV) angular correlation.

α-particle c.m. scattering angle, θ_α (deg)	γ-ray symmetry angle, θ_0 (deg)
15.49	79.2 ± 32.6
16.53	55.1 ± 6.7
17.56	61.1 ± 7.2
19.26	75.5 ± 3.5
20.65	72.7 ± 6.0
21.68	78.2 ± 5.5
23.75	16.0 ± 28.7
24.78	55.0 ± 6.4
25.81	60.8 ± 7.0
26.84	63.1 ± 3.1
28.90	67.5 ± 2.0
30.96	64.4 ± 3.2
33.01	67.3 ± 5.2
35.07	58.2 ± 5.0
37.12	62.0 ± 2.4
39.18	67.8 ± 2.9
41.23	67.4 ± 3.6
43.28	68.9 ± 7.9
45.33	44.8 ± 11.4
47.37	66.5 ± 7.2
49.42	15.7 ± 65.7
51.46	51.7 ± 36.6
53.51	60.1 ± 8.6
55.55	67.8 ± 8.6
59.62	62.1 ± 7.0

A. Carbon 12

Previous calculations on ^{12}C yielded fairly good agreement with experimental data at forward scattering angles.[11] It was found, however, that the optical potential of Ref. 11 (listed as A in Table V) could not adequately describe any of the experimental quantities at α-scattering angles larger than 65°. This is shown in Figs. 8–10. For this reason a new four-parameter potential was sought which would describe all of the data. For this purpose the parameters of Ref. 11 were used as starting values and the computer was asked to optimize the four parameters of a Woods-Saxon potential so as to minimize the quantity χ^2, defined by

$$\chi^2 = \sum_{i=1}^{N} \frac{|\sigma_{\exp}(\theta_i) - \sigma_{th}(\theta_i)|^2}{|\Delta\sigma_{\exp}(\theta_i)|^2},$$

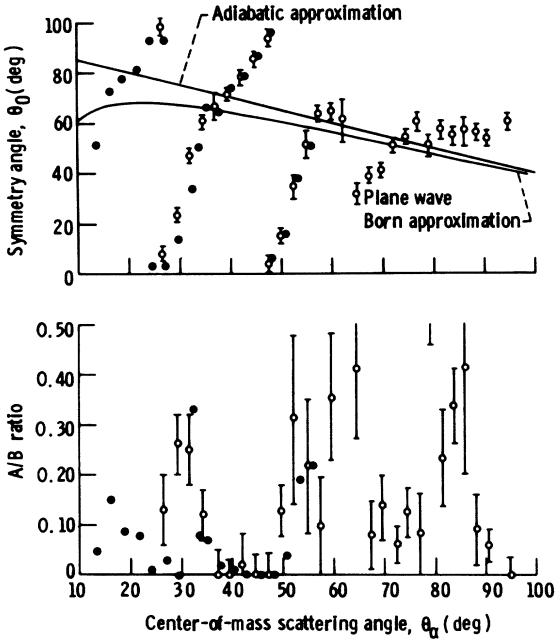

FIG. 4. Experimental results of carbon-12 ($\alpha, \alpha'\gamma$) angular correlation. Solid points are the data of Hendrie (Refs. 10 and 11).

where $\sigma(\theta_i)$ is the elastic cross section at scattering angle θ_i. This process yielded the set of optical-model parameters listed as B in Table V. The fit which these parameters gave for the elastic and inelastic scattering and the angular correlation is also shown in Figs. 8–10. It is clear that although some improvement has been obtained in the description of the elastic and inelastic scattering, that a considerable loss has been suffered in the description of the angular correlation. Because of this, a search was conducted for a new potential unrelated to that proposed for the description of the forward-angle data. This was achieved by fixing the value of the nuclear-radius parameter at a series of discrete values between 1.2 and 2.0 F, and allowing the computer to optimize the three remaining variables. The results of the best of

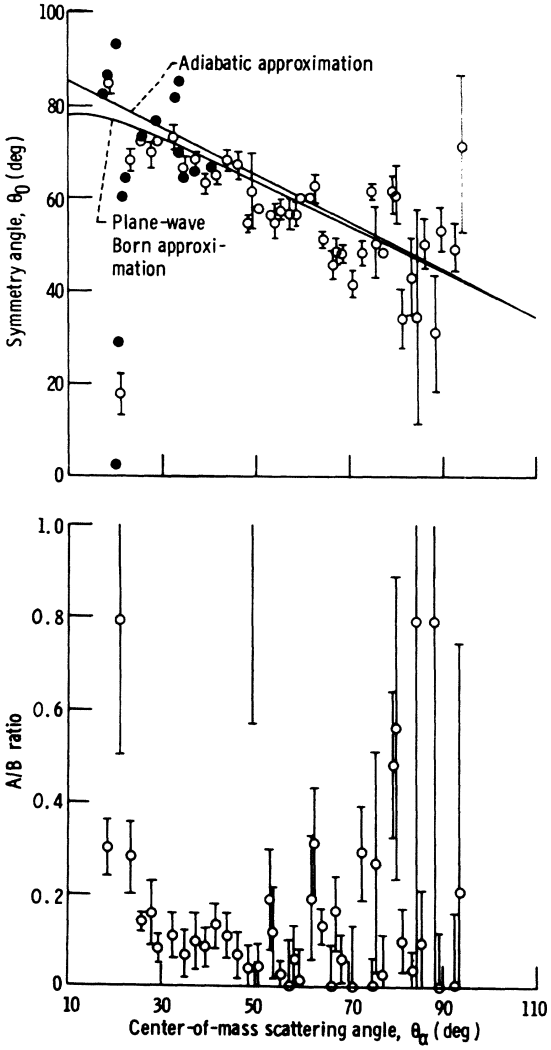

FIG. 5. Experimental results of magnesium-24 $(\alpha, \alpha' \gamma)$ angular correlation. Solid points are the data of Hendrie (Ref. 10).

TABLE V. Results of optical-model calculations for 41-MeV α particles scattered by carbon 12.

Potential	Real potential strength, V (MeV)	Radius constant of real potential, r_0 (F)	Diffuseness of real potential, a_0 (F)	Imaginary potential strength, W (MeV)	Radius constant of imaginary potential, r_i (F)	Diffuseness of imaginary potential, a_i (F)	Goodness of fit per data point, χ^2/N	Total reaction cross section, σ_R (mb)	Nuclear-deformation parameter, β_2
A	24.0	1.99	0.420	13.0	...	...	48.8	927.6	0.89
B	37.16	1.846	0.452	13.27	...	...	20.6	891.2	1.0
C	37.11	1.846	0.451	13.26	...	...	20.6	891.4	1.0
D	199.1	1.262	0.650	42.17	...	...	30.5	963.4	1.6
E	31.46	2.00	0.375	15.78	1.926	0.246	19.8	888.1	0.70

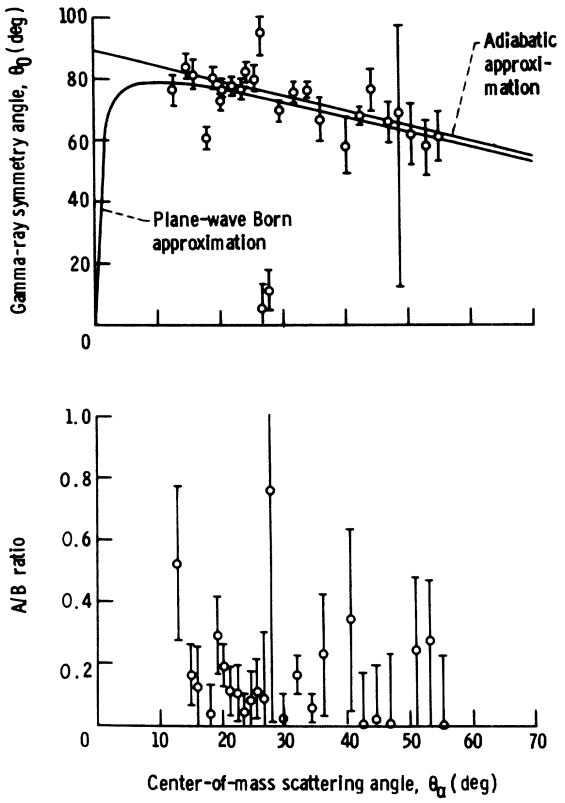

FIG. 6. Experimental results of nickel-58 $(\alpha, \alpha' \gamma)$ angular correlation.

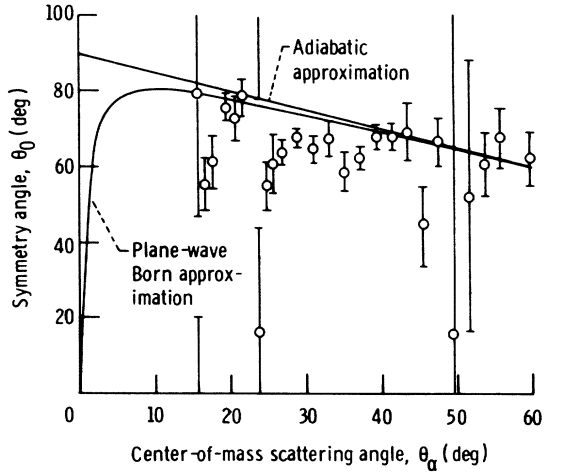

FIG. 7. Experimental results of tin-120 $(\alpha, \alpha' \gamma)$ angular correlation.

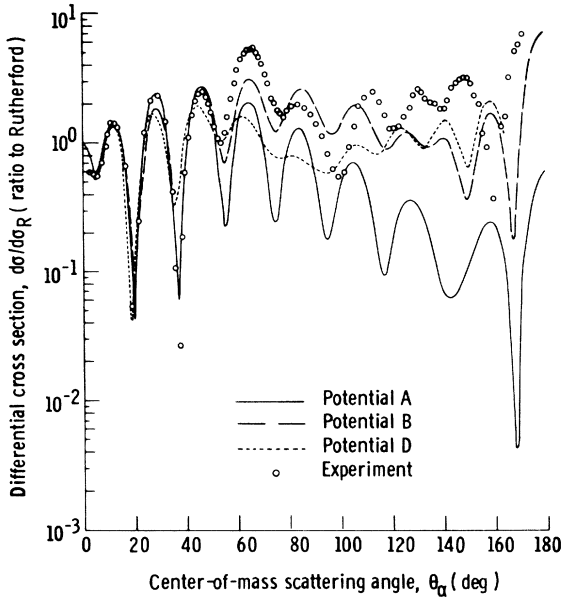

FIG. 8. Experimental and calculated differential cross sections for elastic scattering of 41-MeV α particles from ^{12}C.

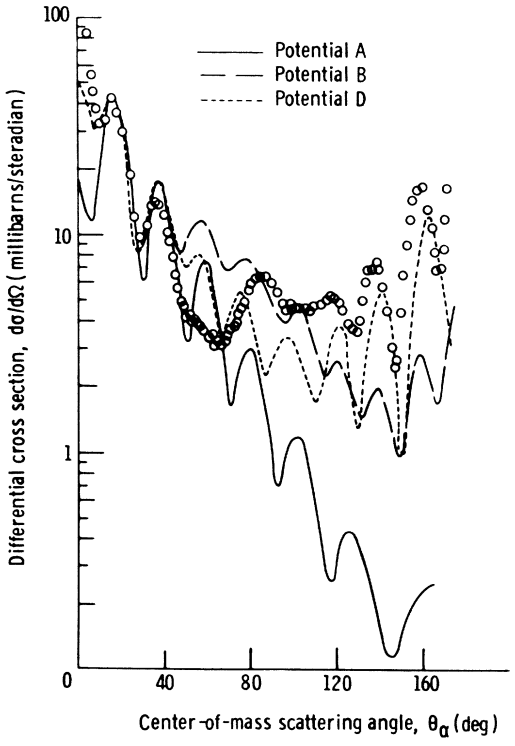

FIG. 9. Experimental and calculated differential cross sections for inelastic scattering ($E^* = 4.433$ MeV) of 41-MeV α particles from ^{12}C.

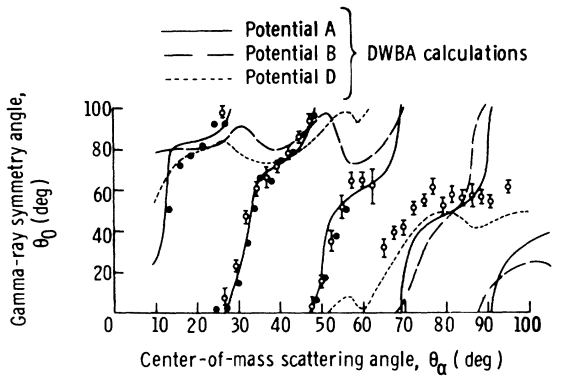

FIG. 10. Experimental and calculated γ-ray symmetry angles for ^{12}C.

these three-parameter problems were then used as starting values for four-parameter searches. The best of these, listed as C in Table V, is virtually identical to potential B.

In addition a number of searches were conducted in which the real well depth was fixed at 150 and 200 MeV, while the nuclear radius was varied in steps of 0.2 F between 1.2 and 2.0 F and the diffuseness and imaginary strength were optimized. The two best of these results were then used as starting values for searches on all four parameters. One such result is listed in Table V as potential D. The results using this deep potential, also shown in Figs. 8–10, were not a significant improvement over the shallower potentials.

Three attempts were made to improve the quality of the fits obtained and still stay within the optical-model DWBA framework. The first involved allowing the optical model to contain six independent parameters; i.e., the radius and diffuseness of the imaginary part of the Woods-Saxon potential were allowed to differ from those of the real part. The best six-parameter potential is listed in Table V as potential E and resulted from starting from the best four-parameter potential. Secondly, in view of the rather large excitation energy (4.433 MeV) of the first excited state of carbon, it seems reasonable to assume that the potential describing the outgoing α particle might differ considerably

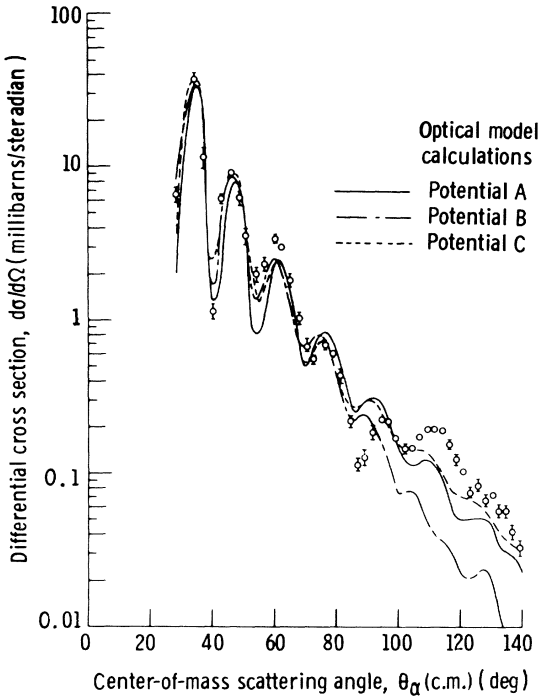

FIG. 11. Experimental and theoretical cross sections for elastic scattering of 42-MeV α particles from ^{24}Mg.

from that required to describe the elastic scattering in the incident channel. In fact, examination of the measured cross section[30] at 35.5 MeV, the energy which corresponds to the velocity of separation of the α particle and the carbon nucleus after an inelastic scattering, would indicate that such is the case. Third, complex coupling was used in the DWBA calculations, with both the real and imaginary parts of the optical potential being deformed.

The results of these three types of calculations were not a great improvement. No matter which device was used the fact seemed to remain that it was impossible to fit both the entire range of cross-section data and the correlation data simultaneously. In general, if one chose a real well depth near 24 MeV (the depth suggested in Ref. 11) then a fairly good fit was obtained to the correla-

TABLE VI. Results of optical-model calculations for 42-MeV α particles scattered by magnesium 24.

Set	Nuclear-radius constant, r_0 (F)	Real potential strength, V (MeV)	Imaginary potential strength, W (MeV)	Diffuseness parameter, a_0 (F)	Goodness of fit per data point, χ^2/N	Total reaction cross section, σ_R (mb)	Nuclear-deformation parameter, β_2
A	1.635	47.05	21.11	0.5613	31.8	1179	0.58
B	1.49	93.64	31.12	0.6190	55.9	1231	0.56
C	1.38	185.7	42.50	0.5753	24.1	1176	0.59

tion data while the cross-section data, particularly at backward angles, was extremely poor. On the other hand if the real well depth were chosen so as to improve the over-all fit to the cross-section data (as with potentials B or C), the fit to the correlation data was poor.

B. Magnesium 24

Optical-model parameters for the description of scattering from ^{24}Mg were obtained by fitting the cross-section data of Vincent, Boschitz, and Priest.[27] A process similar to that described in fitting the carbon-12 data was followed. A series of fixed values was used for one of the parameters (the optical-model radius) and the other three parameters of a four-parameter potential were varied so as to minimize χ^2, which was calculated as in Eq. (6), using only elastic cross-section data. The best of the three-parameter searches then served as a starting potential for a four-parameter search. Three of the potentials obtained are listed in Table VI. The results of cross-section and symmetry-angle calculations are shown with the data in Figs. 11–13. For the inelastic calculations the normalization of theoretical to experimental data was performed at $\theta_\alpha = 40°$ and resulted in equivalent deformation parameters for all of the potentials. These are listed in Table VI and are in agreement with the value previously reported.[31] It is clear that none of the potentials differs significantly from the others in its ability to fit the elastic and inelastic cross sections. This is also true for most of the symmetry-angle calculations. The only real difference is that potential A, with a real well depth of 47.05 MeV predicts a rapid reverse rotation of the symmetry angle at an α-scattering angle of 20°, in agreement with the data. None of the other potentials predicts this rotation. Coincidentally, this potential is quite similar to that selected by Hendrie[10] which in turn was based upon fits to the cross-section data alone.[32,33]

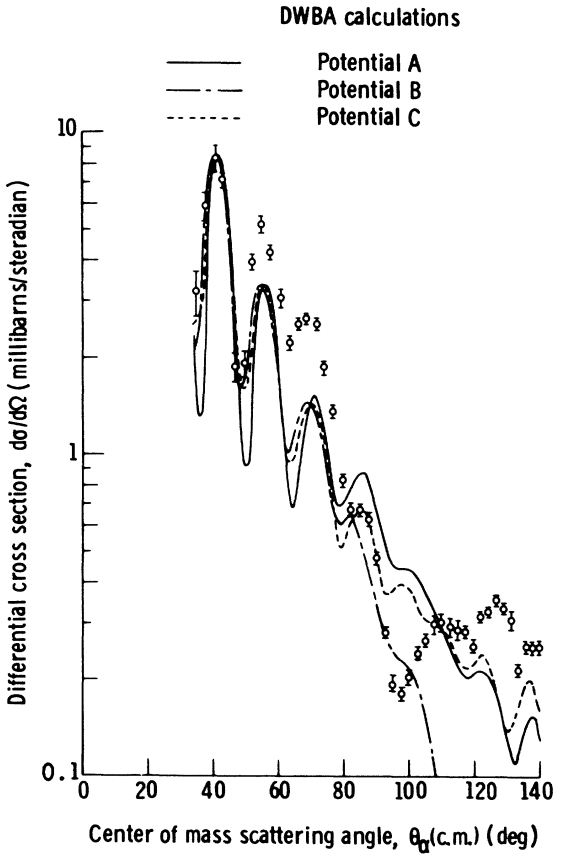

FIG. 12. Experimental and theoretical cross sections for inelastic ($E^* = 1.37$-MeV) scattering of 42-MeV α particles from ^{24}Mg.

C. Nickel 58

A number of four-parameter optical-model searches were performed, using the results of Broek *et al.*[25] The results are listed in Table VII as potentials A, B, and C. The elastic cross section calculated using potential C is shown together with the elastic data in Fig. 14. Potentials A and B yielded results which were qualitatively similar. The fits are good at forward angles but begin to slip out of phase with the data at angles greater than 90°. The inelastic cross section, calculated

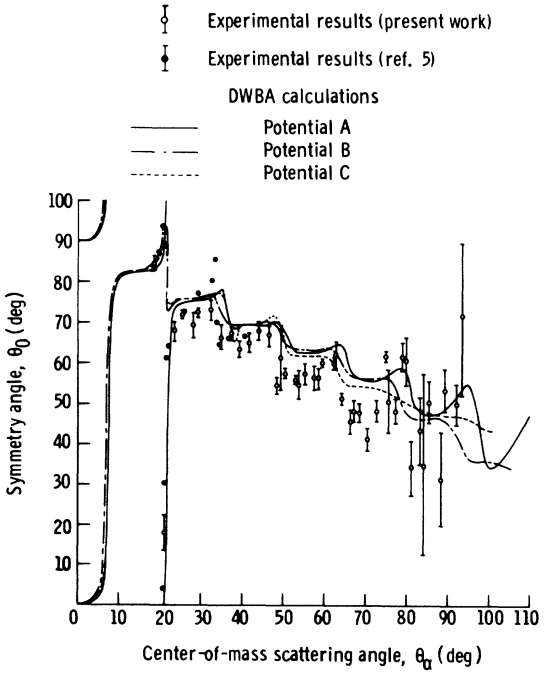

FIG. 13. Experimental and theoretical γ-ray symmetry angles for ^{24}Mg.

using potential C and deforming only the real part to generate a form factor, is shown in Fig. 15. Like the elastic cross section, the fit is good for scattering angles less than approximately 90° but differs in phase from the experimental data at larger angles. Calculations of the inelastic cross section using the other four-parameter potentials yielded similar results although the magnitudes differed slightly at angles larger than 70°. Deformation parameters β_2 were determined by normalizing the calculated angular distribution to the experimental data at 32°. The values obtained are listed in Table VII and are in good agreement with the value of 0.214 ± 0.021 obtained from Coulomb-excitation measurements.[25,34] The angular-correlation symmetry angles calculated using potential C are shown with the experimental data in Fig. 16. It is clear that the symmetry angles are reasonably well described, with rapid reverse rotations being predicted near 17 and 27.5°, as was observed. Unfortunately, all three of the four-parameter potentials predict nearly equivalent symmetry angles, except at scattering angles larger than 45° where the experimental data are too poor to permit a determination of which calculation is better.

In an attempt to improve the fits, calculations were performed using a six-parameter optical potential. In order to determine a six-parameter po-

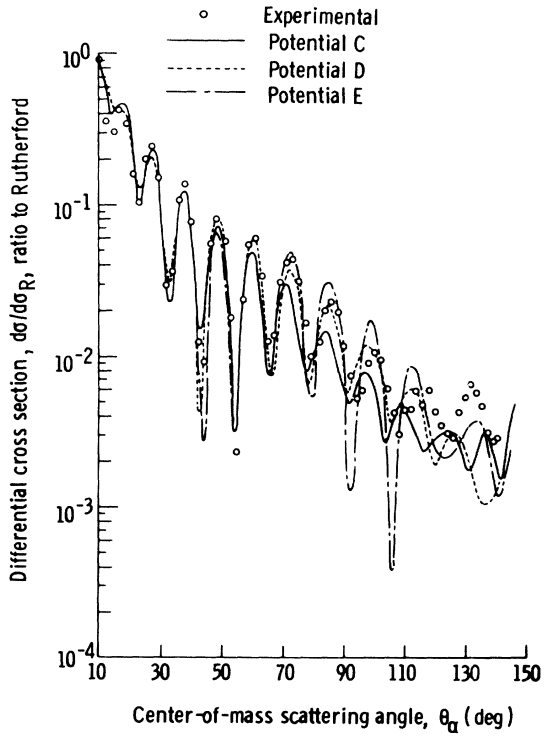

FIG. 14. Experimental and theoretical cross sections for elastic scattering of 42-MeV α particles from ^{58}Ni.

TABLE VII. Results of optical-model calculations for 42-MeV α particles scattered by nickel 58.

Potential	Real potential strength, V (MeV)	Diffuseness of real potential, a_0 (F)	Radius constant of real potential, r_0 (F)	Imaginary potential strength, W (MeV)	Diffuseness of imaginary potential, a_i (F)	Radius constant of imaginary potential, r_i (F)	Total reaction cross section, σ_R (mb)	Goodness of fit per data point χ^2/N	Nuclear-deformation parameter, β_2
A	75.41	0.615	1.48	19.50	...	...	1517	24.0	0.22
B	120.0	0.635	1.39	27.33	...	...	1683	25.9	0.24
C	150.8	0.624	1.36	31.05	...	...	1512	23.2	0.24
D	41.45	0.684	1.52	10.07	0.559	1.71	1541	15.8	0.22
E	139.3	0.565	1.47	16.32	0.275	1.71	1494	16.5	0.25
F	180.8	0.548	1.45	18.63	0.264	1.69	1496	17.2	0.25

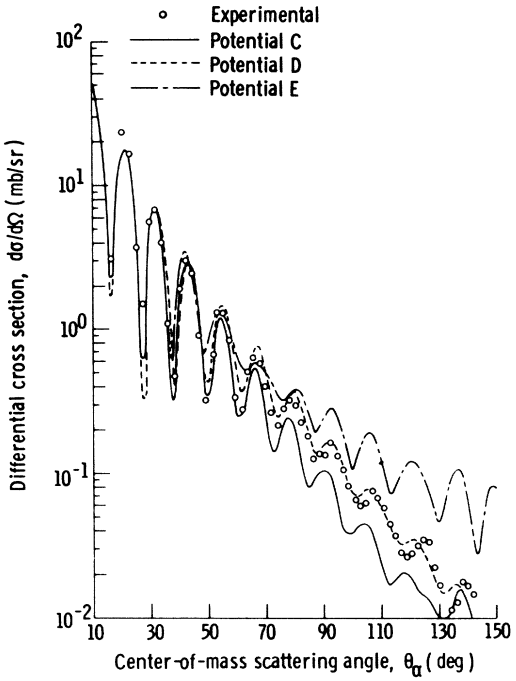

FIG. 15. Experimental and theoretical cross sections for inelastic ($E^*=1.45$ MeV) scattering of 42-MeV α particles from ^{58}Ni.

tential a series of calculations was performed in which the real and imaginary radii were varied in steps of 0.04 F over the range

$$1.31 \leq r_0 \leq 1.75 \text{ F},$$

$$1.43 \leq r_i \leq 1.79 \text{ F}.$$

For each pair of radii the other four parameters were optimized. Three of the potentials which resulted from this procedure are listed in Table VII as D, E, and F. Each of these has an imaginary

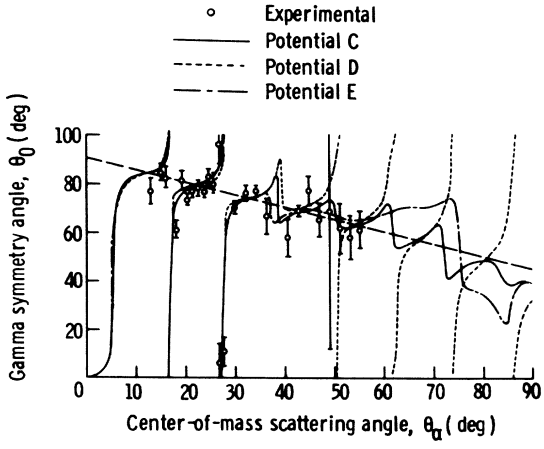

FIG. 16. Experimental and calculated γ-ray symmetry angles for ^{58}Ni.

TABLE VIII. Results of optical-model calculations for 42-MeV α particles scattered by tin 120.

Potential	Real strength, V (MeV)	Radius constant of real potential, r_0 (F)	Diffuseness of real potential, a_0 (F)	Imaginary potential strength, W (MeV)	Radius constant of imaginary potential, r_i (F)	Diffuseness of imaginary potential, a_i (F)	Goodness of fit per data point, χ^2/N	Total reaction cross section, σ_R (mb)	Nuclear-deformation parameter, β_2
A	43.40	1.50	0.710	22.50	...	...	7.3	2023	0.13
B	42.85	1.47	0.724	22.80	1.52	0.605	4.6	1887	0.12
C	52.00	1.48	0.703	24.90	...	...	7.3	2014	0.13
D	51.67	1.44	0.722	25.06	1.50	0.608	4.9	1882	0.13
E	58.00	1.46	0.712	28.00	...	...	7.3	2022	0.14
F	59.34	1.42	0.716	28.38	1.48	0.609	4.7	1880	0.13
G	66.10	1.44	0.710	31.10	...	...	7.3	2012	0.14
H	66.38	1.41	0.716	31.19	1.46	0.608	4.6	1878	0.13
I	87.70	1.40	0.708	38.50	...	...	7.3	2001	0.14
J	87.68	1.37	0.714	38.60	1.43	0.615	5.1	1886	0.13
K	103.00	1.38	0.705	42.60	...	...	7.3	1994	0.14
L	103.14	1.34	0.716	42.83	1.41	0.619	4.7	1878	0.14
M	117.0	1.36	0.707	48.00	...	...	7.6	1993	0.14
N	116.93	1.32	0.716	48.03	1.40	0.615	5.1	1875	0.14
O	316.0	1.19	0.710	145.0	...	...	29.2	1952	0.17
P	316.28	1.18	0.711	145.09	1.26	0.609	5.1	1867	0.15

radius greater than the real radius and an imaginary diffuseness smaller than the real diffuseness, in agreement with the findings of Broek *et al.*[25] The elastic cross sections calculated using D and E are shown in Fig. 14. All three of the six-parameter potentials yield similar values and are significantly better than the four-parameter potentials. In addition, the two deeper six-parameter potentials appear to give a better fit to the large-angle elastic scattering than does the shallow one. The inelastic cross section was calculated using the six-parameter potentials and deforming both the real and imaginary parts to generate the form factor. The results for potentials D and E are shown in Fig. 15. Of the six-parameter potentials, D agrees best with the data although its phase differs slightly from the data at angles larger than 110°. The results of angular-correlation calculations using potentials D and E are shown in Fig. 16. These are virtually identical to the predictions of the four-parameter potentials except at scattering angles beyond 45° where the data are poor.

D. Tin 120

A number of four-parameter optical-model potentials were previously obtained by fitting the ^{120}Sn elastic scattering data.[26] Eight equally good four-parameter potentials were obtained and are listed in Table VIII. Calculations using two of these potentials are compared with the elastic data in Fig. 17. In Fig. 18 the calculated 2^+ cross sections are compared with the experimental values. The DWBA calculations agree with the data over the whole range of potentials, in no way helping to remove the optical-model ambiguities. In Fig. 19 the calculated symmetry angles for the two optical potentials used in Figs. 17 and 18 are compared with the data. All eight of the four-parameter potentials predict nearly identical symmetry angles for α scattering angles larger than 10°. Three of the potentials ($V = 87.7$, 103, and 117 MeV) predict a reverse rotation of the symmetry angle near $\theta_\alpha = 5°$, while the others predict a rapid forward rotation in that region. Beyond 10°, in the region accessible for measurement, all of the potentials tested predicted that the symmetry angle should stay relatively close to the adiabatic prediction. There are small excursions, with the calculation crossing the adiabatic line with a small positive slope at angles that correspond to maxima in the inelastic angular distribution, and with a large negative slope at angles that correspond to minima in the inelastic 2^+ cross section. None of the po-

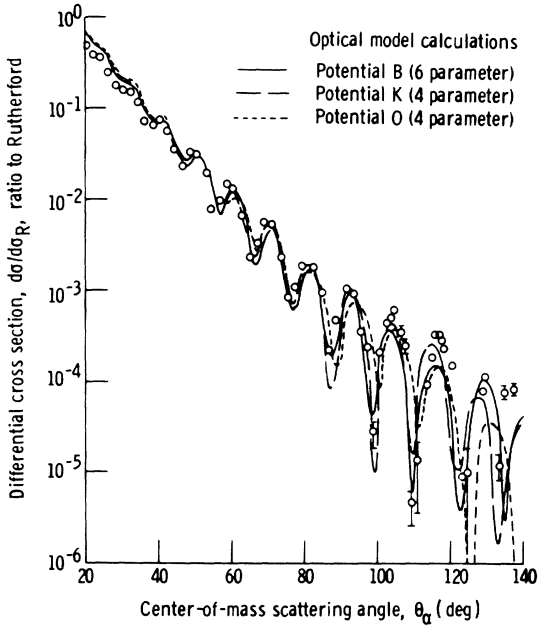

FIG. 17. Experimental and theoretical cross sections for elastic scattering of 42-MeV α particles from ^{120}Sn.

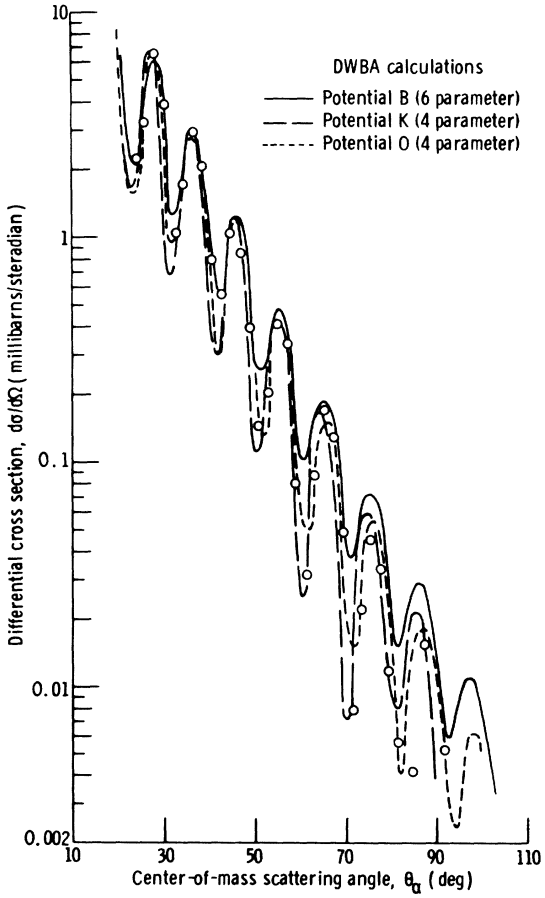

FIG. 18. Experimental and theoretical cross sections for inelastic ($E^* = 1.176$ MeV) scattering of 42-MeV α particles from ^{120}Sn.

tentials were able to predict the rapid rotations in the symmetry angle which are seen experimentally near 16 and 24°.

In an attempt to better fit the correlation data, a six-parameter optical potential was used. The six-parameter potentials were found by using the four-parameter potentials as starting points and allowing the optical-model program to optimize all six parameters. The potentials which resulted from this procedure are listed in Table VIII, and one calculation is compared with the data in Fig. 17. As in the calculations for ^{58}Ni, the optimum imaginary radii were larger than the real radii, while the imaginary diffusenesses were smaller than the real diffusenesses. The results of using one of the six-parameter potentials in complex-coupling DWBA calculations are shown in Figs. 18 and 19. The fits to the inelastic data show a slight improvement. In particular, at large angles the peaks in the cross section have been shifted to slightly larger angles resulting in better agreement. The calculated symmetry angles, however, are essentially identical in every case to those obtained using a four-parameter potential to describe the scattering.

V. COUPLED-CHANNELS CALCULATIONS

Coupled-channels calculations were performed only for the ^{12}C data. This seemed reasonable in view of the exceptionally large strength of the first excited (4.433-MeV, 2^+) state of ^{12}C. The program used for the calculations was the extended optical-model (EOM) code of Wills.[32] The calculations treated the 4.433-MeV state as either the first member of a rotational or vibrational spectrum. In the case of a vibration, some calculations were done which coupled the 7.65-MeV state as well, treating it as the 0^+ member of a two-phonon group. Calculations which coupled in a third member of a rotational band were not performed, since for the most likely candidate[35] (14.08 MeV, 4^+) no α-scattering data were available. It was found that the coupled-channels calculations did not differ significantly from the DWBA results. This is similar to Satchler's results[36] for 46-MeV protons scattered from ^{12}C. Also, as found by Satchler, it makes little difference in the 2^+ cross section whether one assumes a vibrational or rotational excitation.

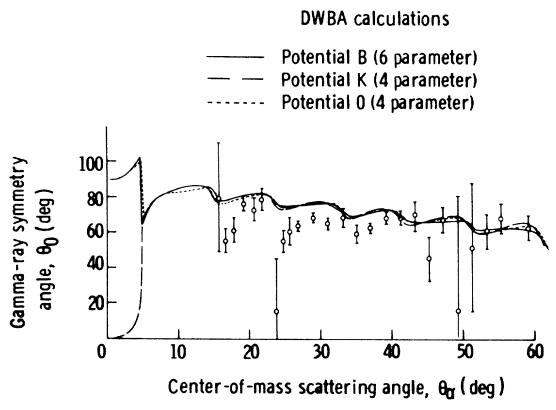

FIG. 19. Experimental and theoretical γ-ray symmetry angles for ^{120}Sn.

VI. DISCUSSION

One of the purposes of this study was to determine whether it would be possible to remove the optical-potential ambiguities ordinarily found when fitting 42-MeV α-scattering data. For the angular-correlation data over the range of α-scattering angles which we have studied, the answer seems to be no. However, examination of the individual isotopes seems to be worthwhile.

The difficulties encountered in fitting α scattering from carbon and magnesium are of a different nature from those found in nickel and tin. In the lighter nuclei it was not possible to find any potential which gave a satisfactory description of the elastic and inelastic scattering cross sections. The reasons for the failure of optical-model descriptions have been discussed elsewhere.[37] The result of the failure, in any case, is that for carbon and magnesium the "resolution of ambiguities" can be no more than the selection of one poorly fitting potential rather than another.

For ^{12}C it appears that the optical potentials may be divided into two sets. One set, derived to fit the forward-angle cross-section data, yields a fair description of the angular-correlation data. The second set, derived to fit cross-section data over a wide angular range, gives extremely poor fits to the correlation data.

^{24}Mg was the only nucleus of the four studied for which one optical potential yielded a better description of the angular-correlation data than did the

TABLE IX. Comparison of rotations in symmetry-angle data. Values of the nuclear radius used in this table are obtained by fitting Blair's expression (Ref. 7) to the experimentally measured elastic cross section.

Nucleus	Last rotation in symmetry angle, θ_{max} (deg)	Scattering-angle argument, $kR_0 \sin\frac{1}{2}\theta_{max}$
^{12}C	47	8.6
^{24}Mg	20	5.0
^{58}Ni	28	8.7
^{120}Sn	24	9.0

others tested. Of the numerous potentials which gave equivalent fits to the elastic and inelastic scattering cross sections, only one potential, $V = 47.05$ MeV, was able to predict the existence of the experimentally observed rapid reverse rotation of the correlation pattern near $\theta_\alpha = 20°$. At all other α-scattering angles all of the potentials gave nearly identical results.

For the two heavier nuclei, real ambiguities exist. For each nucleus a variety of optical potentials can be found which describe both the elastic and inelastic cross-section data fairly well. Unfortunately, virtually all such potentials predict identical correlation patterns. Consequently, one must conclude that the measurement of in-plane angular correlations, at least over the angular range studied here, is of little use in resolving such ambiguities. Although variations in the predicted correlation patterns do occur at large scattering angles and at extreme forward angles, experimental difficulties preclude data collection at these angles. This inability to eliminate ambiguities is probably an indication that, as for the cross section, the correlation function is sensitive only to the gross features of the nuclear potential, as was suggested by Verhaar and Tolsma (Ref. 16), who were able to reproduce the general behavior of the symmetry angle merely by allowing the ring locus of a diffraction model to have finite width.

The correlation data obtained, however, do indicate that at least at large angles a more detailed explanation is required than that of Verhaar and Tolsma or any of the other simplified models proposed for the purpose of explaining correlation data. In particular, both Verhaar and Tolsma[16] and Wills and Cramer[15] predict a symmetry angle which will continue to rotate indefinitely; while experimentally, in every case, the rotation was found to cease beyond some α-scattering angle θ(max). In fact, in three of the four isotopes the angle at which the last rotation occurred corresponded to nearly the same value of the scattering argument[7] $kR_0 \sin\frac{1}{2}\theta$. This is shown in Table IX.

One other conclusion may be drawn from the present work. The behavior of the symmetry angle appears to be completely independent of any details of the nuclear structure. For the four cases studied here, two (^{58}Ni and ^{120}Sn) are generally considered to be spherical nuclei with the first excited state represented as a vibrational excitation. For magnesium, on the other hand, the first 2^+ state is generally thought of as the first member of a rotational band, while the structure of the first excited state of ^{12}C is not very well understood, although it has been suggested[35] that it may also be the 2^+ member of a rotational band. At any rate, the four nuclei studied certainly exhibit a variety of structures, and yet the nature of the angular-correlation data is virtually identical for all four. This is experimentally equivalent to the findings of Wold,[38] who found that calculated symmetry angles are quite insensitive to variations in microscopic nuclear wave functions.

VII. ACKNOWLEDGMENTS

The authors wish to thank Professor W. Eidson for several helpful and interesting discussions during the experimental phase of this work, R. C. Braley for his assistance in carrying out the calculations, and Dr. D. L. Hendrie for having read the manuscript.

[1]G. Bruge, J. C. Faivre, H. Faraggi, and A. Bussiere, Nucl. Phys. A146, 597 (1970).
[2]A. M. Bernstein, in *Advances in Nuclear Physics*, edited by M. Baranger and E. Vogt (Plenum Press, Inc., New York, 1969), Vol. III.
[3]A. Bohr, Nucl. Phys. 10, 486 (1959).
[4]J. G. Cramer, Jr., and W. W. Eidson, Nucl. Phys. 55, 593 (1964).
[5]G. R. Satchler, Proc. Phys. Soc. A68, 1037 (1955).
[6]J. S. Blair and L. Wilets, Phys. Rev. 121, 1493 (1961).
[7]J. S. Blair, Phys. Rev. 115, 928 (1959).
[8]W. W. Eidson, J. G. Cramer, Jr., D. E. Blatchley, and R. D. Bent, Nucl. Phys. 55, 613 (1964).
[9]J. G. Cramer, Jr., W. W. Eidson, and D. E. Blatchley, Argonne National Laboratory Report No. ANL-6848, 153, 1964 (unpublished).
[10]D. L. Hendrie, Ph.D. thesis, University of Washington, 1964 (unpublished).
[11]D. K. McDaniels, D. L. Hendrie, R. H. Bassel, and G. R. Satchler, Phys. Letters 1, 295 (1962).
[12]G. Igo, Phys. Rev. 115, 1665 (1959).
[13]N. Austern, Ann. Phys. (N.Y.) 15, 299 (1961).
[14]R. M. Drisko, G. R. Satchler, and R. H. Bassel, Phys. Letters 5, 347 (1963).
[15]J. G. Wills and J. G. Cramer, Jr., Argonne National Laboratory Report No. ANL-6848, 147, 1964 (unpublished).
[16]B. J. Verhaar and L. D. Tolsma, Nucl. Phys. A90, 612 (1967).
[17]R. F. Leonard, W. M. Stewart, N. Baron, and R. C. Braley, National Aeronautics and Space Administration Report No. NASA TN D-4683, 1968 (unpublished).
[18]W. M. Stewart, N. Baron, R. C. Braley, and R. F. Leonard, National Aeronautics and Space Administration Report No. NASA TN-D-5568, 1969 (unpublished).
[19]N. Baron, R. Leonard, and W. M. Stewart, National Aeronautics and Space Administration Report No. NASA TN D-5585, 1970 (unpublished).
[20]R. F. Leonard, W. M. Stewart, and N. Baron, National Aeronautics and Space Administration Report No. NASA TN D-5569, 1969 (unpublished).

[21]M. K. Banerjee and C. A. Levinson, Ann. Phys. (N.Y.) 2, 499 (1957).
[22]M. E. Rose, Phys. Rev. 91, 610 (1953).
[23]I. M. Naqib, Ph.D. thesis, University of Washington, 1962 (unpublished).
[24]A. I. Yavin and G. W. Farwell, Nucl. Phys. 12, 1 (1959).
[25]H. W. Broek, J. L. Yntema, B. Buck, and G. R. Satchler, Nucl. Phys. 64, 259 (1965).
[26]N. Baron, R. F. Leonard, J. L. Need, W. M. Stewart, and V. A. Madsen, Phys. Rev. 146, 861 (1966).
[27]J. S. Vincent, E. T. Boschitz, and J. R. Priest, Phys. Letters 25B, 81 (1967).
[28]M. A. Melkanoff, J. S. Nodvik, D. S. Saxon, and D. G. Cantor, *A FORTRAN Program for Elastic Scattering Analysis with the Nuclear Optical Model* (University of California Press, Berkeley, California, 1961).
[29]W. R. Gibbs, V. A. Madsen, J. A. Miller, W. Tobocman, E. C. Cox, and L. Mowry, National Aeronautics and Space Administration Report No. NASA TN D-2170, 1964 (unpublished).
[30]T. Mikumo, J. Phys. Soc. Japan 16, 1066 (1961).
[31]P. H. Stelson and L. Grodzins, Nucl. Data A1, 21 (1965).
[32]J. G. Wills, Ph.D. thesis, University of Washington, 1963 (unpublished).
[33]E. Rost, Phys. Rev. 128, 2708 (1962).
[34]P. H. Stelson and F. K. McGowan, Nucl. Phys. 32, 652 (1962).
[35]D. K. Scott, P. M. Portner, J. M. Nelson, A. C. Shotter, A. J. Mitchell, N. S. Chant, D. G. Montague, and K. Ramaratarам, Nucl. Phys. A141, 497 (1970).
[36]G. R. Satchler, Nucl. Phys. A100, 497 (1967).
[37]P. E. Hodgson, *The Optical Model of Elastic Scattering* (Oxford University Press, Oxford, England, 1963).
[38]D. C. Wold, Bull. Am. Phys. Soc. 15, 1656 (1970).

PHYSICAL REVIEW C VOLUME 4, NUMBER 4 OCTOBER 1971

Applicability of the Constant-Nuclear-Temperature Approximation in Statistical-Model Calculations of Neutron Cross Sections at 14.4 MeV for Medium-Z Nuclei*

Wen-deh Lu† and R. W. Fink

School of Chemistry, Georgia Institute of Technology, Atlanta, Georgia 30332

(Received 21 December 1970)

Cross sections of $(n,2n)$, (n,p), and (n,α) reactions of medium-Z nuclei at 14.4 MeV, calculated from the statistical model with the constant-nuclear-temperature approximation for level densities, are compared with experiment. Using effective thresholds for second- and third-emitted neutrons, obtained by adding 0.5 and 1 MeV to the ground-state thresholds, respectively, the agreement with experiment is about ±15, ±20, and ±30% for $(n,2n)$, (n,p), and (n,α) reactions, respectively. For (n,α) reactions, it is necessary to add 1 MeV to the pairing energy for the shell closures at $N=50$ and 82 to get satisfactory agreement. An average nuclear temperature of 1.5 MeV is used for all types of reactions and for all nuclei investigated. The exponential dependence on $(N-Z)/A$ for (n,p) cross sections in Levkovskii's empirical formula is derived from the statistical model and a semiempirical mass equation. Empirical equations are obtained which depend only on A and Z for quick estimation of 14.4-MeV $(n,2n)$ cross sections from $Z=28$ to 82 and of $[(n,np)+(n,pn)+(n,d)]$ cross sections of the lightest stable isotope of even-Z elements in the region of $Z=28$ to 50.

I. INTRODUCTION

In previous papers[1-4] we have reported $(n,2n)$, (n,p), and (n,α) cross sections of medium-Z nuclei at 14.4 MeV which are compared with the predictions of Pearlstein[5] and of Levkovskii[6] for $(n,2n)$ and (n,p) reactions, respectively. In both cases, the agreement between prediction and experiment is satisfactory. However, in Pearlstein's method a normalization function is used to obtain absolute $(n,2n)$ cross sections, while Levkovskii's formula for (n,p) cross sections is entirely empirical. The normalization function used by Pearlstein depends on the value of the experimental cross sections and on the form of the function assumed. The physical significance of the normalization function is not clear.[7]

In the present work, the applicability of the constant-nuclear-temperature approximation in statistical-model calculations of neutron cross sections at 14.4 MeV for medium-Z nuclei is demonstrated. It is shown that the exponential dependence on $(N-Z)/A$ for (n,p) cross sections in Levkovskii's empirical formula may be derived from the statistical model with a constant-nuclear-temperature approximation for level densities and a semiempirical mass formula. In addition, some empirical equations which are functions of A and Z only are obtained which are useful for quick estimation of 14.4-MeV $(n,2n)$ cross sections in the region of

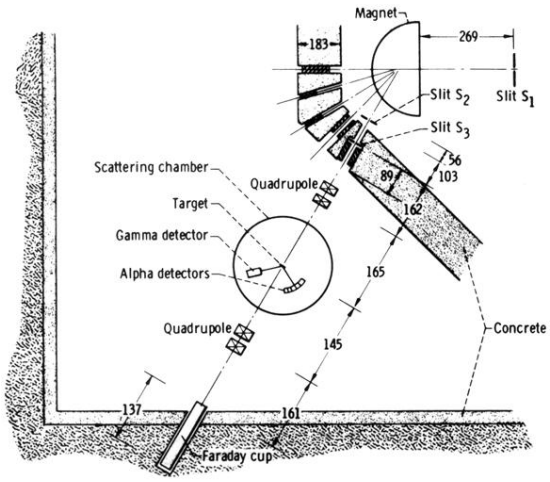

FIG. 1. Schematic diagram of scattering system.
(All dimensions are in cm.)